

Promotion of Cortical Neurogenesis from the Neural Stem Cells in the Adult Mouse Subcallosal Zone

JOO YEON KIM,^a KYUHYUN CHOI,^b MOHAMMED R. SHAKER,^a JU-HYUN LEE,^a BORAM LEE,^a EUNSOO LEE,^a JAE-YONG PARK,^c MI-SUN LIM,^{d,e} CHANG-HWAN PARK,^{d,e,f} KI SOON SHIN,^b HYUN KIM,^a DONGHO GEUM,^g WOONG SUN^a

^aDepartment of Anatomy and Division of Brain Korea 21 Plus Biomedical Science and ^bDepartment of Biomedical Sciences, Korea University College of Medicine, Seoul, Korea; ^bDepartment of Biology, Department of Life and Nanopharmaceutical Sciences, Kyung Hee University, Seoul, Republic of Korea; ^cSchool of Biosystem and Biomedical Science, College of Health Science, Korea University, Seoul, Republic of Korea; ^dGraduate School of Biomedical Science and Engineering; ^eHanyang Biomedical Research Institute; ^fDepartment of Microbiology, College of Medicine, Hanyang University, Seoul, Korea

Correspondence: Woong Sun, Ph.D., Department of Anatomy, Korea University College of Medicine, Anam-dong, Seongbuk-gu, Seoul 136-705, Korea. Telephone: 822-2286-1404; Fax: 822-929-5696; e-mail: woong-sun@korea.ac.kr; or Dongho Geum, Ph.D., Department of Biomedical Sciences, Korea University College of Medicine, Anam-dong, Seongbuk-gu, Seoul 136-705, Korea. Telephone: 822-2286-1091; Fax: 822-924-6324; e-mail: geumd@korea.ac.kr

Received May 31, 2015; accepted for publication November 17, 2015; first published online in *STEM CELLS EXPRESS* December 23, 2015.

© AlphaMed Press
1066-5099/2016/\$30.00/0

<http://dx.doi.org/10.1002/stem.2276>

Key Words. Subcallosal zone • Traumatic brain injury • Adult neurogenesis • Adult neural stem cells • Brain-derived neurotrophic factor • Bcl-xL

ABSTRACT

Neurogenesis occurs spontaneously in the subventricular zone (SVZ) of the lateral ventricle in adult rodent brain, but it has long been debated whether there is sufficient adult neurogenesis in human SVZ. Subcallosal zone (SCZ), a posterior continuum of SVZ closely associated with posterior regions of cortical white matter, has also been reported to contain adult neural stem cells (aNSCs) in both rodents and humans. However, little is known whether SCZ-derived aNSC (SCZ-aNSCs) can produce cortical neurons following brain injury. We found that SCZ-aNSCs exhibited limited neuronal differentiation potential in culture and after transplantation in mice. Neuroblasts derived from SCZ initially migrated toward injured cortex regions following brain injury, but later exhibited apoptosis. Overexpression of anti-apoptotic *bcl-xL* in the SCZ by retroviral infection rescued neuroblasts from cell death in the injured cortex, but neuronal maturation was still limited, resulting in atrophy. In combination with Bcl-xL, infusion of brain-derived neurotrophic factor rescued atrophy, and importantly, a subset of such SCZ-aNSCs differentiated and attained morphological and physiological characteristics of mature, excitatory neurons. These results suggest that the combination of anti-apoptotic and neurotrophic factors might enable the use of aNSCs derived from the SCZ in cortical neurogenesis for neural replacement therapy. *STEM CELLS* 2016;34:888–901

SIGNIFICANCE STATEMENT

Mammalian subcallosal zone (SCZ), or subcortical white matter, contains neural stem cells (NSCs), but they normally produce glial cells. By combination of anti-apoptotic gene delivery and neurotrophic factors, mature cortical neurons were produced from adult SCZ, suggesting the potential use of SCZ NSCs for cortical neurogenesis-based brain repair.

INTRODUCTION

Neural stem cells (NSCs) are enriched in the adult rodent neurogenic regions including the subventricular zone (SVZ) of the lateral ventricle and subgranular zone of the dentate gyrus, where new neurons are spontaneously produced. Several other regions in the brain, such as the cerebral cortex, amygdala, hypothalamus, and substantia nigra, have also been reported to contain NSCs which maintain the quiescent status in the normal brain [1]. Interestingly, NSCs in such neurogenic or non-neurogenic areas can be activated and generate new neural cells in response to brain injury [2, 3]. Several studies have shown that brain damage following ischemia and trauma promotes neurogenesis from SVZ and recruit

newly generated neuroblasts toward the injured area [4–7]. Furthermore, inducing apoptosis of cortical neurons could recruit immature cells into mature neural circuits [8, 9]. New cells produced in adult brain may differentiate into mature neurons and integrate into existing neuronal circuits, but spontaneous neuronal maturation is often limited [10, 11]. Therefore, the use of NSCs in neural repair requires developing strategies to not only enhance survival but also promote differentiation of NSCs.

The limited pool of stem cells in the human SVZ has raised a concern regarding the potential use of adult NSCs (aNSCs) derived from subcallosal zone (SCZ) (SCZ-aNSCs) [12, 13]. In contrast to the highly active, rodent SVZ-aNSCs, which continuously provide new

neurons to the olfactory bulb and mediate neural plasticity [14, 15], adult neurogenesis in the human olfactory bulb is much less pronounced. Recently, we and others have revealed that the SCZ is also a region that produces neuroblasts [8, 16]. The SCZ is developmentally originated from the posterior aspects of the lateral ventricle and is closely associated with the white matter. aNSCs in the SCZ appear to provide oligodendrocytes in the white matter during postnatal development, but SVZ-aNSCs also spontaneously generate immature neuroblasts [8, 16–18]. We reported that such spontaneously produced neuroblasts in the SCZ were eventually, executed by Bax-dependent apoptosis [8]. Interestingly, it has been reported that human or primate SCZ or temporal lobe-associated white matter, whose developmental origin is similar to the rodent SCZ, also contain aNSCs, suggesting the potential use of SCZ-aNSCs in brain repair [19–24].

Traumatic brain injury (TBI) is one of the most prevalent causes of death and prolonged disability in modern society. Accidental loss of neurons is frequently associated with permanent impairment of brain functions, and poor recovery is due to the limited repair mechanisms that promote neuronal replacements. Intriguingly, it has been shown that SCZ-aNSCs can respond to brain injury, resulting in the production of new cells including neuroblasts in mice [8, 24]. Especially, SCZ-aNSCs selectively responded to the posterior brain damage, suggesting that SCZ-aNSCs contributes to the posterior brain repair [8]. While neuroblasts that migrate to neurogenic regions, such as hippocampus, appear to survive and differentiate into mature neurons [24], it is yet unclear whether SCZ-derived neuroblasts, which migrate to non-neurogenic regions, such as cerebral cortex, can survive and mature. To evaluate the potential use of the SCZ-aNSCs in brain repair, we explored their neurogenic potential in multiple models including in vitro culture, cell transplantation, and selective labeling and lineage tracing of endogenous SCZ-derived neuroblasts following brain injury. While newly produced neuroblasts failed to survive on their own, combination of retroviral over-expression of an anti-apoptotic gene *bcl-xL*, and microinfusion of brain-derived neurotrophic factor (BDNF) promoted maturation of SCZ-derived neurons and integration into neural circuits, suggesting SCZ-aNSCs as a potential source of cells for brain repair.

MATERIALS AND METHODS

aNSC Culture

Adult male C57BL/6 (8–9 weeks old) mice were obtained from ORIENT BIO (Seongnam, Korea). All experiments were carried out in accordance with the regulations and approval of the Animal Care and Use Committee of the Korea University. After section of adult mouse brain into 1-mm slices, the SVZ and SCZ tissues were isolated and incubated with a digestion buffer containing 0.8% papain (Worthington, Lakewood, NJ) and 0.08% dispase II (Roche Applied Science, Indianapolis, IN, USA) in HBSS for 45 minutes at 37°C [17]. Anatomical regions where we used for SVZ and SCZ NSCs were shown in Figure 1A and Supporting Information Figure 2A–2C. Dissociated cells were seeded and maintained as neurospheres in an ultra-low attachment surface six-well dish in Dulbecco's modified Eagle's medium/F12 media containing 1% N2, 2% B27,

penicillin–streptomycin, supplemented with basic fibroblast growth factor (20 ng/ml, Invitrogen, Carlsbad, CA, USA), and epidermal growth factor (20 ng/ml, Invitrogen, Carlsbad, CA, USA). Neurospheres over 50 μm diameter were included for further analyses. To maintain the aNSCs as monolayer, we coated six-well dish with poly-D-lysine and laminin. After neurospheres were dissociated into individual cells with Accutase (Innovative Cell Technologies, San Diego, CA, USA) for 5–10 minutes at 37°C, dissociated cells were seeded in a density 5×10^5 cells per six-well. Luna-FL automated cell counter (Logos Biosystems, Korea) was used for the quantification of total cell number, and routinely >95% cell viability was obtained. To assess differentiation potential, we seeded 1×10^5 cells per 18-mm cover slip coated with poly-D-lysine and laminin and maintained without growth factors for 6 days.

Animal Treatments

To perform cryogenic TBI, mice were anesthetized by pentobarbital (50 mg/kg) and then placed in stereotaxic instrument. After sagittal scalp incision, a magnetic probe (5-mm diameter), which was prechilled in liquid nitrogen, was placed on the right skull where we target such as SCZ (anterior, +2.7 mm; medial, –2.0 mm; relative to Bregma) for 30 seconds, as described earlier [8]. The skin was sutured, and the animals were placed on a 37°C hot plate until they were awake. Mice were killed at indicated time points. For stereotaxic injection of retrovirus, mice were deeply anesthetized by injecting pentobarbital (50 mg/kg) and placed on a stereotaxic device (Stoelting, Wood Dale, IL). For viral infection, we adjusted the virus to 1×10^9 transducing units per milliliter, and green fluorescent protein (GFP)- or Bcl-xL-retrovirus (1.5–2 μl) was injected into the right SCZ (Anterior to posterior (AP): –2.7 mm, Medial to lateral (ML): –2.7 mm; Dorsal to ventral (DV): –1.3 mm relative to Bregma) using a 30-gauge microsyringe at a rate of 0.5 $\mu\text{l}/\text{minute}$. One day after retroviral injection, animals received TBI at the hindbrain level, a procedure known to promote migration of SCZ-derived neuroblasts to the injured brain area [8]. For the infusion of BDNF (20 ng/ μl , Invitrogen, Carlsbad, CA), microcannula (World Precision Instruments, Inc. Sarasota) was inserted into the injured cortex (DV = 1 mm) and mounted with cement. Schematic diagram for the anatomical locations of viral injection, TBI, and cannulation is summarized in Supporting Information Figure 7. Efficient diffusion of the injected solution to the injured cortical regions was visually validated by trypan blue injection (Supporting Information Fig. 7C). BDNF was then injected once per 3 days for 1 month. For the lineage tracing of atrophied cells, tamoxifen (10 mg/day, Sigma-Aldrich, St. Louis, MO, USA) was injected for 5 days after Bcl-xL injection into DCX-tamoxifen-dependent Cre recombinase (*creER*)^{T2} mice, and the mice were killed 30 days later. Detailed procedure for the production of DCX-*creER*^{T2} is provided in Supporting Information Materials. We excluded three animals from our experiments due to the unexpected surgery-induced death or detachment of cannula.

Transplantation

Adult NSCs from the SVZ (SVZ-aNSCs) and SCZ (SCZ-aNSCs) on passage 1–2 (P1–P2) were dissociated into single cells and infected with GFP-retrovirus. At 4 days after infection, the

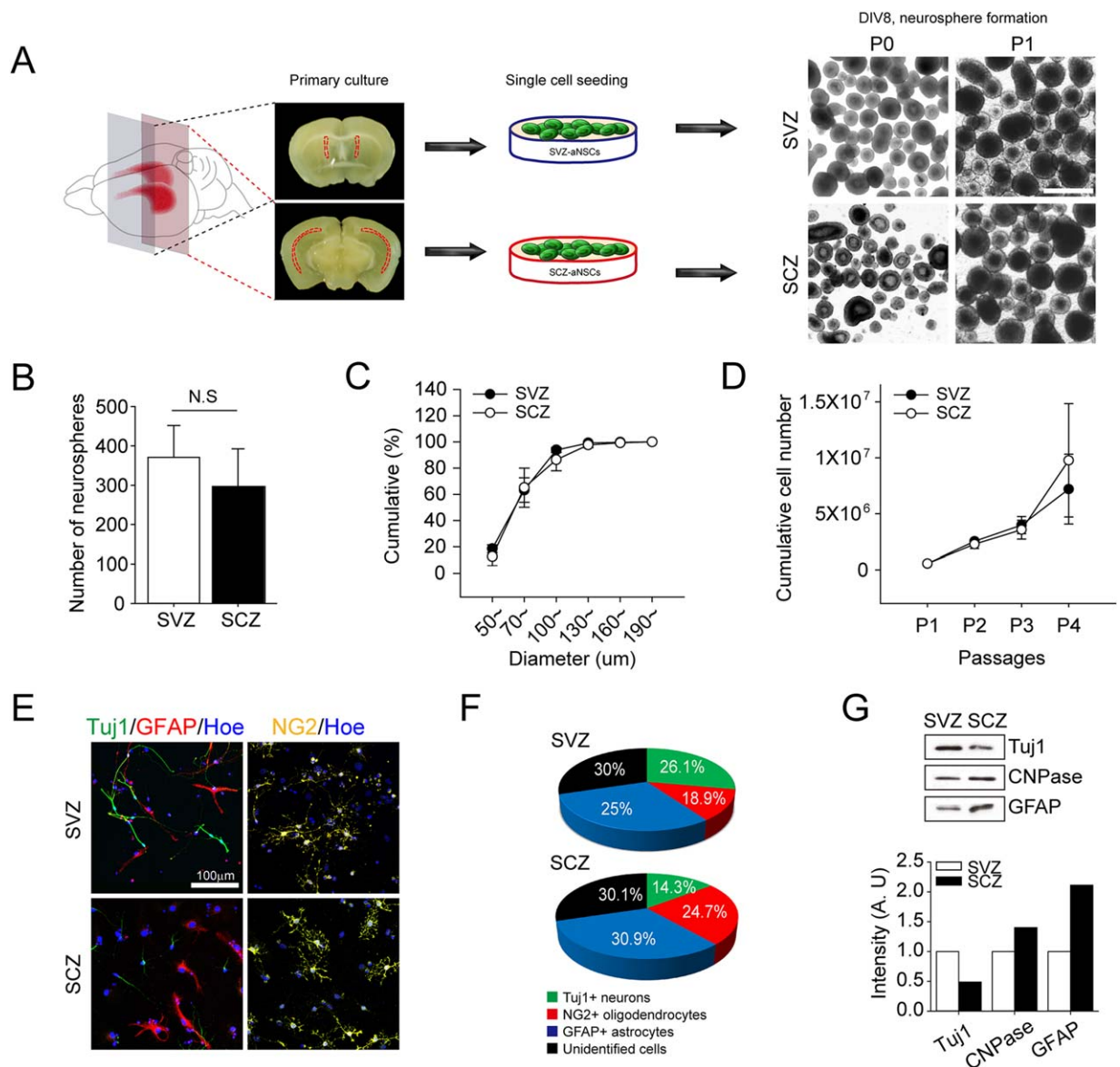


Figure 1. Proliferation and differentiation potentials of subventricular zone (SVZ)- and subcallosal zone (SCZ)-derived aNSCs in vitro. **(A):** Schematic diagram for SVZ- and SCZ-derived aNSCs culture. Representative images of neurospheres produced in primary cultures from the SVZ (upper panel) or SCZ (lower panel) at passages 0 (P0) and P1 are shown. Scale bar = 500 μm. **(B):** Quantification of the number of neurospheres at P1 (Number per well after seeding 500,000 dissociated NSCs). Data are expressed as mean ± SEM ($n = 10$ dishes for cell counting). Student's t test. **(C):** Cumulative distribution of the diameter of neurospheres obtained from SVZ or SCZ at P1. **(D):** Growth curves of neurospheres obtained from SVZ or SCZ during the passages of NSCs. **(E):** Representative images of monolayer cultures from SVZ- or SCZ-derived cells immunostained for TuJ1 (neuronal marker), NG2 (oligodendrocyte marker), and glial fibrillary acidic protein (GFAP) (astrocyte marker) as indicated. Nuclei were counter-stained with Hoechst 33342 (blue). Scale bar = 100 μm. **(F):** Phi-charts showing the percentage of cells labeled with the indicated markers. **(G):** Representative immunoblots of SVZ- or SCZ-derived monocultures probed for anti-TuJ1, 2',3'-cyclic nucleotide 3'-phosphodiesterase, and GFAP antibodies as indicated. Cells were lysed after 6 days of differentiation in vitro. Experiment was duplicated and similar result was obtained. Quantification of the band intensity was shown in the graph below. Values were normalized by re-blotting of each membrane with beta-actin antibody. Abbreviations: CNPase, 2',3'-cyclic nucleotide 3'-phosphodiesterase; GFAP, glial fibrillary acidic protein; SCZ, subcallosal zone; SVZ, subventricular zone.

expression of GFP was examined and typically >95% of cells exhibited GFP expression. GFP-labeled aNSC (2.5×10^5 per microliter to $2 \mu\text{l}$) were then collected in artificial cerebrospinal fluid (aCSF) solution (Tocris, Missouri, USA), and injected into the SVZ (AP: +0.2 mm, ML: -1.4 mm, DV: -2.2 mm to Bregma) or the SCZ (AP: -0.27 mm, ML: -0.27, DV: -0.13) by a 27-gauge microsyringe at a rate of $0.5 \mu\text{l}/\text{minute}$. Mice were killed and subjected to analysis at 9 days after transplantation.

For the quantification of the grafted cell number, every sixth sections of serially cut ($40 \mu\text{m}$) brain slices were visually inspected, and all sections containing GFP+ cells were used for the quantification. To calculate total number of grafted cells in each animal, summation of counted cells from all sections was multiplied by fraction factor ($\times 6$), and stereologically corrected using Abercrombie methods [4, 25–27].

Histology

For immunohistochemical analysis, mice were perfused with 4% paraformaldehyde (PFA) and the brains were isolated. Following post-fixation in the 4% PFA overnight, brains were cryoprotected in 30% sucrose until the brains sank and then sectioned serially (40 μ m). Every 6th or 12th section containing SCZ was blocked with 3% bovine serum albumin in phosphate-buffered saline (PBS) for 30 minutes. Primary antibodies were then applied to the sections overnight at room temperature. Primary antibodies used in this study were rabbit anti-gial fibrillary acidic protein (GFAP) (1:1,000; DAKO, Glostrup, Denmark), mouse anti-2',3'-cyclic nucleotide 3'-phosphodiesterase (CNPase) (1:500; Sigma-Aldrich, St. Louis, MO, USA), Goat anti-DCX (1:500; Santa Cruz Biotechnology, Santa Cruz, CA USA), mouse anti-neuronal nuclei (NeuN) (1:1,000; Millipore, Billerica, MA), rabbit anti-Olig2 (1:500; IBL, Takasaki, Japan), rabbit anti-Tuj1 (1:1,000–2,000; Sigma-Aldrich, St. Louis, MO, USA), rabbit anti-myelin basic protein (MBP) (1:500; Millipore, Billerica, MA), rabbit anti-MAP2 (1:1,000; Millipore, Billerica, MA), rabbit anti-active caspase 3 (1:500; Cell Signaling Technology, Danvers, MA, USA), rabbit anti-Cux1 (1:150; Santa Cruz Biotechnology, Santa Cruz, CA USA), rabbit anti-C-Fos (1:500; Santa Cruz Biotechnology, Santa Cruz, CA USA), mouse anti-vGlut (1:500; Synaptic Systems, Goettingen, Germany), rabbit anti-TBR2 (1:500; Abcam, Cambridge, UK), rabbit anti-Tuj1 (1:500; Sigma-Aldrich, St. Louis, MO, USA), rabbit anti-NG2 (1:500; Millipore, Billerica, MA), and chick anti-GFP (1:1,000; Abcam, Cambridge, UK). After several washes with PBS, sections were incubated with appropriate secondary antibodies for 30 minutes. Nuclei were then counterstained with Hoechst33342, and the images were captured with a Zeiss LSM510 and LSM700 confocal microscope (Carl Zeiss, Goettingen, Germany).

Electrophysiological Analysis

For slice preparation, mice were deeply anesthetized with Zylazine and Zolazepam and transcardial perfusions were performed with 20 ml of ice-cold carbogenated aCSF of the following composition (in mM): 124 NaCl, 2.5 KCl, 1.2 NaH₂PO₄, 24 NaHCO₃, 5 HEPES, 13 glucose, 2 MgSO₄, 2 CaCl₂. (pH 7.3–7.4). Mice were then decapitated and the brains were collected into ice-cold carbogenated aCSF. Brains were mounted for coronal sectioning at 300 μ m thickness on a VT1000S (Leica, German). Slice were initially recovered for <15 minutes at 32°C in carbogenated protective cutting buffer of the following composition (in mM): 92 cholinchloride, 2.5 KCl, 1.2 NaH₂PO₄, 30 NaHCO₃, 20 HEPES, 25 glucose, 5 sodium ascorbate, 2 thiourea, 3 sodium pyruvate, 10 MgSO₄, 0.5 CaCl₂ (pH 7.3–7.4). After initial recovery period, the slices were transferred into a holding chamber containing carbogenated aCSF for 1 hour (room temperature). Slices were then transferred to the recording chamber of a BX51WI microscope (Olympus). Slices were fully submerged at a flow rate of 1.6 ml/minute, and maintained at 30 \pm 1°C. Whole-cell recording were made using an EPC10 amplifier (HEKA Elektronik). Signals were sampled at 10 kHz. Patch-pipettes were pulled (Narishige Sci. Instrument Lab.) from borosilicate glass and had a tip resistance of 5–6 M Ω when filled with pipette solution. The pipette solution contained (in mM): 100 K-gluconate, 20 KCl, 10 mM HEPES, 0.2 EGTA, 10 2Na⁺ phosphocreatine, 4 Mg²⁺ ATP, 0.3 Na⁺ GTP; pH

was adjusted to 7.2 with KOH. The holding potential was –70 mV for Excitatory postsynaptic potential (EPSC).

Statistical Analysis

Statistical significance of differences between the groups was evaluated by independent sample *t* tests. All the analyses were carried out with SPSS software, and all values are given as mean \pm SEM. A *p* < 0.05 were considered statistically significant.

RESULTS

Limited Neurogenic Potential of the SCZ-Derived aNSCs In Vitro

It has been suggested that aNSCs in different areas of the SVZ are a diverse, heterogeneous population of progenitors, which exhibit distinct potential to proliferate and differentiate [28]. To examine the proliferative and differential potentials of the aNSCs derived from SCZ (SCZ-aNSCs), we dissected out the SCZ region and cultured the cells to induce the formation of neurospheres and compared with aNSCs derived from SVZ (SVZ-aNSCs). SCZ-aNSCs produced fewer neurospheres than SVZ-aNSCs (Fig. 1A; Supporting Information Fig. 1A, 1B) (SVZ: 381 \pm 12.7 vs. SCZ: 128 \pm 14.6 neurospheres, *p* < 0.001), and the total number of cells from SCZ-aNSCs was also significantly less than that of SVZ-aNSCs (SVZ: 3.73 \times 10⁶ \pm 5.38 \times 10⁵ vs. SCZ: 7.98 \times 10⁵ \pm 2.43 \times 10⁵ cells, *p* < 0.001) (Supporting Information Fig. 1A, 1C), showing that SCZ contains less aNSCs than SVZ that can survive and proliferate in our culture condition. However, after passage 1, neurospheres derived from SCZ and SVZ were similar in number and size (Fig. 1A–1C), and growth curves from proliferating cells derived from SCZ and SVZ were also similar at low and high passages (Fig. 1D), suggesting that SCZ harbor aNSCs that proliferate as potently as the SVZ-aNSCs in vitro.

We then compared the potential of aNSCs from the two different regions for differentiation. When cells were allowed to differentiate spontaneously for 6 days in vitro, less cells from SCZ-aNSCs differentiated into TuJ1⁺ neurons than those from SVZ-aNSCs (SVZ: 26.1 \pm 2.87% vs. SCZ: 14.34 \pm 1.91%, *p* < 0.004). More cells from SCZ-aNSCs differentiated into NG2⁺ pre-oligodendrocytes (SVZ: 18.9 \pm 1.05% vs. SCZ: 24.7 \pm 1.44%, *p* < 0.007), and aNSCs from the two regions produced similar number of GFAP⁺ astrocytes (SVZ: 25 \pm 1.9% vs. SCZ: 30.9 \pm 1.93%, not significant) (Fig. 1E, 1F). Immunoblot analysis using specific markers further confirmed the reduced neurogenic but enhanced gliogenic potential of the SCZ-aNSCs as compared to SVZ-aNSCs (Fig. 1G).

Differential Neurogenic Potential of the aNSCs Following Transplantation

To test the in vivo fate of SCZ- and SVZ-aNSCs, SCZ- or SVZ-derived aNSCs were first infected with retrovirus carrying GFP in vitro, and 4 days later, the same number of aNSCs (2.5 \times 10⁵ cells per microliter) was transplanted into either the SCZ or the SVZ region of adult mice (Fig. 2A). When we examined the grafted cells in their original or altered environments after 9 days, the grafted cells were found in their injected sites as clusters but with significant dispersions into the nearby host brain area (Fig. 2B). Compared with SVZ-

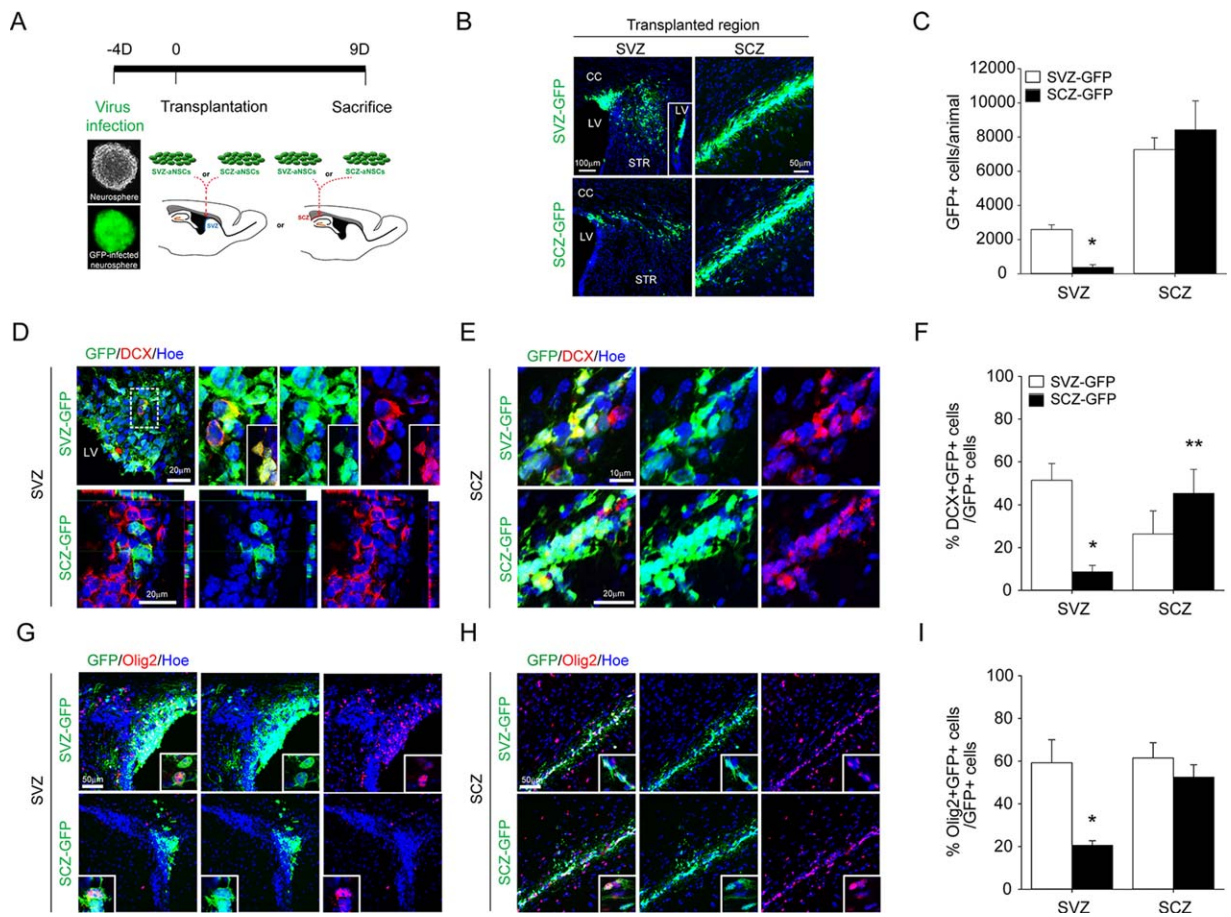


Figure 2. Fate of transplanted subventricular zone (SVZ)- or subcallosal zone (SCZ)-derived adult neural stem cells (aNSCs) in the host SVZ or SCZ. **(A):** Experimental scheme of viral injection, transplantation, and analysis. aNSCs derived from SVZ or SCZ were transfected with retrovirus-green fluorescent protein (GFP) and then transplanted into either SVZ or SCZ. Fate of the transfected GFP-aNSCs was examined 9 days after transplantation. **(B):** Representative images of GFP-aNSCs derived from either SVZ (SVZ-GFP) or SCZ (SCZ-GFP) transplanted in the host SVZ or SCZ. Brains were sectioned and imaged at 9 days after transplantation of aNSCs. **(C):** Total number of grafted cells in each animal. **(D, E):** Representative images of transplanted SVZ-GFP (upper panel) and SCZ-GFP (lower panel) in the host SVZ (D) and SCZ (E). Sections were immunostained for DCX. Dashed box in (C) is enlarged in right. Insets in (D) in left show dispersed neuroblasts. **(F):** Quantification of the grafted-DCX⁺GFP⁺ cells in host SVZ and SCZ. Data are expressed as mean \pm SEM ($n = 5$), *, $p < 0.05$, Student's t test (*, SVZ-GFP vs. SCZ-GFP in the SVZ; **, SVZ-GFP vs. SCZ-GFP in the SCZ). **(G, H):** Representative images of transplanted SVZ-GFP (upper panel) and SCZ-GFP (lower panel) in the host SVZ (G) and SCZ (H). Sections were immunostained for Olig2. Insets show enlarged images from other section. **(I):** Quantification of the grafted-Olig2⁺GFP⁺ cells in the SVZ and SCZ. Data are expressed as mean \pm SEM ($n = 5$), *, $p < 0.05$, Student's t test (*, LV, lateral ventricle; STR, striatum; CC, corpus callosum, SVZ-GFP vs. SCZ-GFP in the SVZ). Abbreviations: DCX, Doublecortin; GFP, green fluorescent protein; SCZ, subcallosal zone; SVZ, subventricular zone.

aNSCs (SVZ-GFP), SCZ-aNSCs (SCZ-GFP) formed noticeably smaller clusters in the SVZ (Fig. 2B). However, in the SCZ, both SCZ- and SVZ-GFP were widely dispersed along the injected area (Fig. 2B). The total number of grafted cells from SCZ that survived in the SVZ was much less comparing with that from SVZ (SVZ-GFP: 2585.5 ± 274.3 , $n = 5$ vs. SCZ-GFP: 374.6 ± 160.3 , $n = 5$), raising a possibility that SCZ-derived NSCs cannot be maintained well in the ectopic location (Fig. 2C). On the other hand, substantially larger number of grafted cells survived after transplanted to the SCZ, but there was no difference in survived cell numbers in two groups (SVZ-GFP: 7270.2 ± 693 , $n = 5$ vs. SCZ-GFP: 8425.2 ± 1688.4 , $n = 5$). These results suggest that the maintenance of the grafted cells was dependent on the environment, as well as the origin of the transplanted cells.

When we examined the proportion of neural progenitors, we found that nestin-expressing progenitors were similar in SVZ and

SCZ regions (Supporting Information Fig. 2D–2F). Interestingly, in the SVZ, SCZ-GFP produced less neuroblasts (Fig. 2D–2F) and oligodendrocytes (Fig. 2G–2I), as compared to SVZ-GFP, whereas astrocytic differentiation was comparable (Supporting Information Fig. 2G–2I). In the SCZ, SCZ-GFP and SVZ-GFP produced similar proportions of neuroblasts (Fig. 2D–2F), oligodendrocytes (Fig. 2G–2I), and astrocytes (Supporting Information Fig. 2G–2I). These results suggest that SCZ-aNSCs exhibit neurogenic and gliogenic potential in their native environment but weaker neurogenic and oligodendrogenic potential in the altered environment.

Fate of SCZ-Derived Cells in the Cerebral Cortex After Cryptogenic TBI

Accumulating evidence suggests that brain injury enhances neurogenesis in the SVZ and DG [2, 29–31]. As aNSCs found in other brain regions, endogenous aNSCs in the SCZ can also be stimulated by TBI of posterior brain regions [8]. To

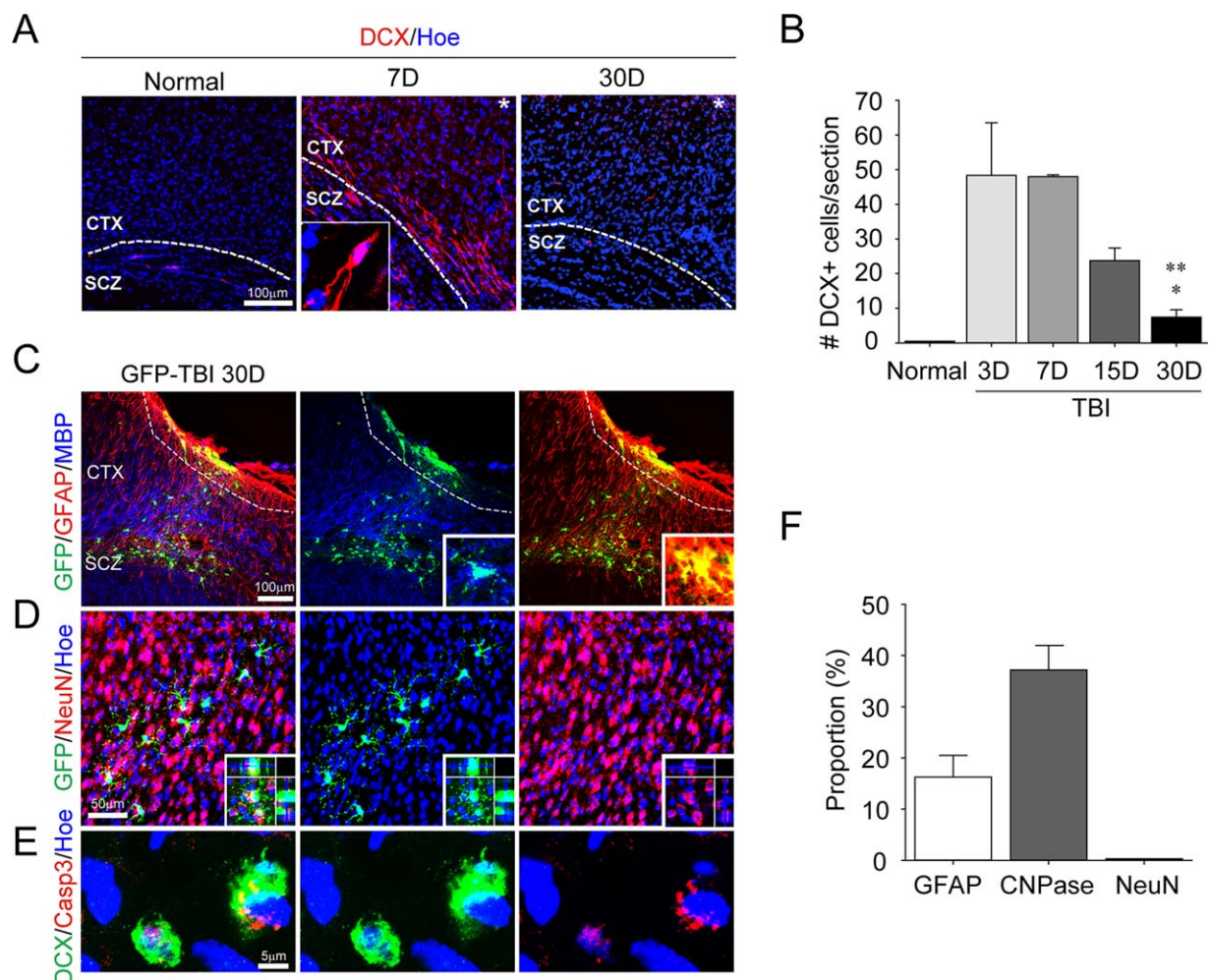


Figure 3. Fate of subcallosal zone (SCZ)-derived adult neural stem cells (aNSCs) after traumatic brain injury (TBI). **(A):** Distribution of DCX⁺ neuroblasts in control and injured brains. Brains were examined at 7 (7D) and 30 days (30D) after TBI, as indicated. Nuclei were counter-stained with Hoechst33342 (Hoe) in blue. Dotted lines indicate the border between the SCZ and cortex region (CTX). BOX in the middle panel indicates magnified individual neuroblast. Scale bar = (A) 100 μ m. **(B):** Quantification of DCX⁺ neuroblasts in control and injured brain. Data are expressed as mean \pm SEM ($n = 5$), *, $p < 0.05$, Student's t test. (*, TBI3D vs. TBI30D; **, TBI7D vs. TBI30D). **(C):** Three days before TBI, aNSCs derived from SCZ were infected with green fluorescent protein-expressing retrovirus. Shown are representative images of injured brains sectioned from animals killed at 30 days after TBI. Sections were immunostained for glial fibrillary acidic protein (GFAP) and myelin basic protein as indicated. Insets show enlarged images of single cells. Scale bar = 100 μ m. **(D):** Sections were immunostained for NeuN. Insets show enlarged images of single cells. **(E):** Dying neuroblasts in the injured cortex. Fifteen days after TBI, activated caspase 3 was detected in several DCX-expressing neuroblasts. Scale bar = (E) 5 μ m. **(F):** Quantification of cell fate of the NSCs from the SCZ 30 days after TBI. Mice were killed 30 days after TBI, and brain sections were immunostained for GFAP, 2',3'-cyclic nucleotide 3'-phosphodiesterase, or NeuN, as indicated. Data are expressed as mean \pm SEM ($n = 6$). Abbreviations: CNPase, 2',3'-cyclic nucleotide 3'-phosphodiesterase; CTX, cortex; DCX, Doublecortin; GFAP, glial fibrillary acidic protein; GFP, green fluorescent protein; MBP, myelin basic protein; SCZ, subcallosal zone; TBI, traumatic brain injury.

evaluate the extent of injury-induced neuroblast formation and migration in response to posterior brain damage, changes in the number of neuroblasts were examined in the injured cerebral cortex after cryogenic TBI. TBI was applied to the posterior cerebral cortex (visual cortex), a procedure that has been shown to promote the migration of neuroblasts generated from the SCZ [8]. Consistent with our previous report, DCX-expressing cells markedly increased in the injured cerebral cortex when observed at 3 days after injury, and the increase was maintained for a week (TBI 3D: 48.4 ± 15.1 , TBI 7D: 48 ± 0.5 , $n = 5$). However, the number of neuroblasts was progressively reduced and returned to basal level by 30 days after TBI (TBI 15D: 23.8 ± 3.6 , TBI 30D: 7.4 ± 2.1 , $n = 5$) (Fig. 3A, 3B). Results from the time course analysis raise two possibilities

that either neuroblasts underwent apoptosis or they differentiated into mature neurons with a loss of DCX-immunoreactivity.

To trace the fate of newly produced endogenous SCZ-derived cells in the cerebral cortex, GFP-expressing retrovirus was focally injected into the SCZ before application of TBI, and we examined the fate of GFP-expressing cells 30 days thereafter. Interestingly, double labeling of GFP with markers for specific cell types revealed that SCZ-derived astrocytes were mainly localized at the glial scar area, whereas oligodendrocytes derived from SCZ were widely dispersed in the injured cortex regions (Fig. 3C; Supporting Information Fig. 5). Quantification of the cell types demonstrated that largest proportion ($37.2 \pm 4.8\%$) of cells were double-labeled with CNPase or MBP, markers for oligodendrocytes, and a small proportion

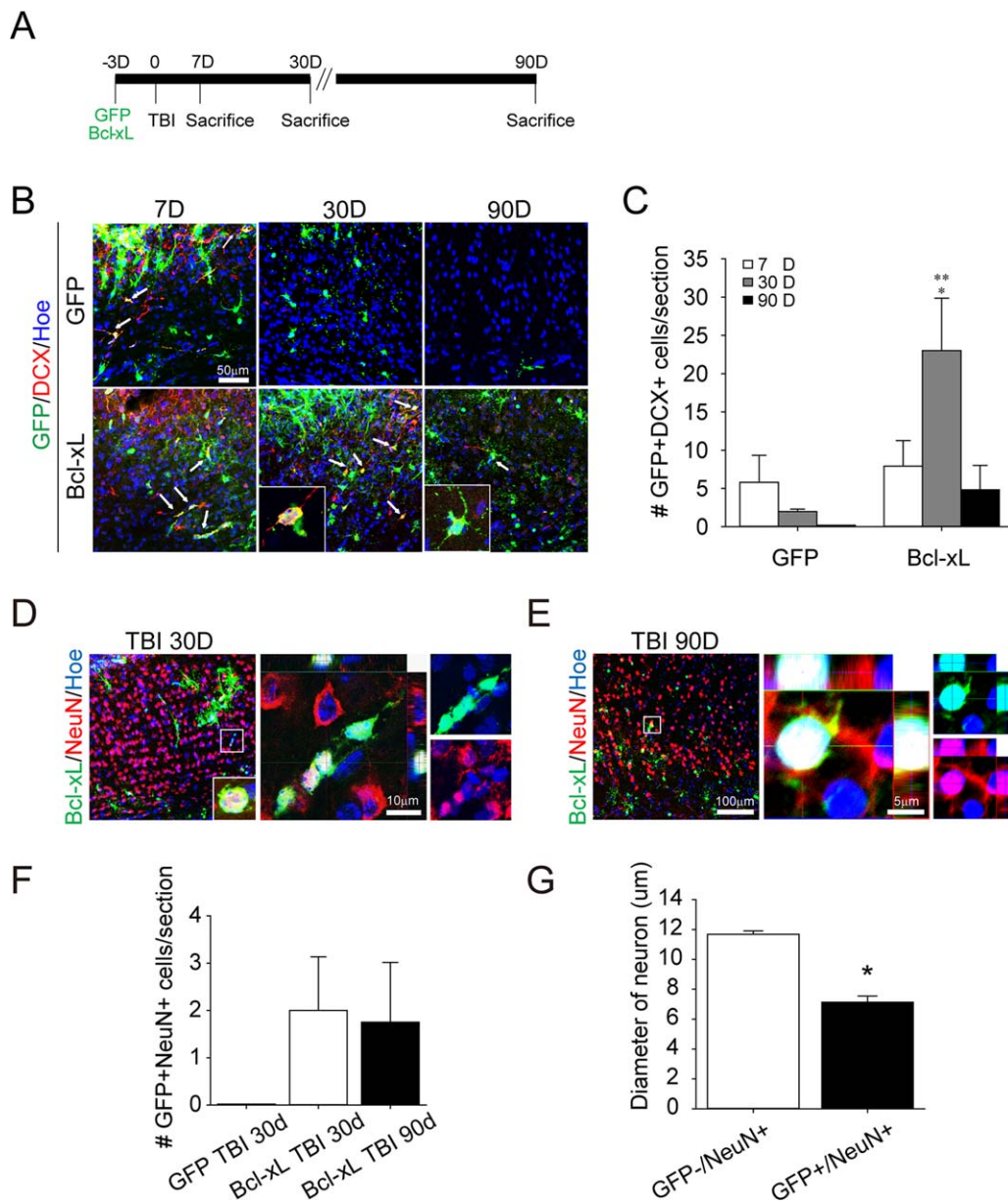


Figure 4. Bcl-xL overexpression increased the number of neuroblasts and formed mature neuron. **(A):** Experimental scheme of transfection (green fluorescent protein [GFP] or GFP-Bcl-xL), traumatic brain injury (TBI), and analysis. GFP- or GFP-Bcl-xL-expressing retrovirus was injected into subcallosal zone (SCZ) and the animals were subject to TBI 3 days later. Mice were killed for analysis at 7 (7D), 30 (30D) and 90 days (90D) after TBI, as indicated. **(B):** Representative images of injured brains that had been transfected with either GFP- or GFP-Bcl-xL-expressing retrovirus. Insets are magnified images of DCX⁺/GFP⁺ double-positive cells. Nuclei were counter-stained with Hoechst 33342 (blue). Arrow means colocalized cells with DCX. **(C):** Quantification of DCX⁺ cells in GFP- or GFP-Bcl-xL-expressing cells. Data are expressed as mean \pm SEM ($n = 4$ for GFP group, $n = 6$ for Bcl-xL group), *, $p < 0.05$, Student's t test. (*, GFP 30D vs. GFP-Bcl-xL 30D; **, GFP-Bcl-xL 7D vs. GFP-Bcl-xL 30D). **(D, E):** Representative images of brain sections immunostained for a mature neuron marker, NeuN (red), and GFP (green) at 30 **(D)** or 90 days **(E)** after TBI. Note that GFP-Bcl-xL-infected cells differentiated into mature neurons in the injured cortex. Cells transfected with GFP-Bcl-xL-expressing retrovirus expressed NeuN in the SCZ after TBI (inset). Magnified images on the right are shown in color split pattern. Nuclei were counter-stained with Hoechst 33342 (blue). **(F):** Quantification of NeuN⁺ cells in brain sections from mice infected with GFP- or GFP-Bcl-xL-expressing retrovirus at 30 or 90 days after TBI. **(G):** Quantification of the diameter of NeuN⁺/GFP⁺ cells in the injured cortex. Data are expressed as mean \pm SEM ($n = 4$ for GFP group, $n = 6$ for Bcl-xL group). *, $p < 0.05$, Student's t test. Abbreviations: DCX, Doublecortin; GFP, green fluorescent protein; TBI, traumatic brain injury.

(16.3 \pm 4.2%) was labeled with GFAP (Fig. 3F). However, GFP-expressing cells never expressed NeuN, a marker for mature neurons (Fig. 3D, 3F), and other mature neuronal markers, such as MAP2 and Tuj-1, were also undetectable in GFP-expressing cells (Supporting Information Fig. 3). These results favor the pos-

sibility that young neuroblasts produced in the injured cerebral cortex underwent apoptosis. Supporting this notion, activated caspase 3 was readily detected in DCX-expressing neuroblasts (Fig. 3E). These results are in fact consistent with our recent report suggesting that aNSCs in the SCZ fail to survive [8]

Overexpression of Antiapoptotic Gene *bcl-xL* Increased the Number of Neuroblasts After TBI

To examine whether neuroblasts can be rescued from apoptotic cell death, retrovirus expressing an anti-apoptotic gene *bcl-xL* was introduced into the SCZ (Fig. 4A). Seven days after TBI, similar numbers of DCX⁺ cells were found in the injured cerebral cortex of both GFP- and Bcl-xL-virus-infected groups ($5.8 \pm$ vs. 7.9 ± 3.3 cells per section) (Fig. 4B, 4C). However, when observed at 30 days after TBI, the number of DCX⁺ cells was markedly enhanced in the Bcl-xL-injected group, whereas DCX⁺ neuroblasts were substantially reduced in the control group (21.8 ± 7.1 vs. 2 ± 0.3 cells per section) (Fig. 4B, 4C). By 90 days after TBI, however, the number of DCX⁺ cells in the Bcl-xL group substantially decreased (2.3 ± 6.8 cells per section) (Fig. 4B, 4C), suggesting that Bcl-xL-overexpressing, DCX⁺ neuroblasts lost their DCX expression during the 30- to 90-day period.

It has been demonstrated that overexpression of Bcl-xL can enhance neuronal differentiation of embryonic cortical neural precursors [32]. Therefore, we tested whether Bcl-xL affect neuronal differentiation. However, when SCZ-aNSCs were cultured to undergo spontaneous differentiation for 6 days, SCZ-aNSCs overexpressing Bcl-xL and control SVZ-aNSCs expressing GFP produced TuJ1⁺ neurons to similar extent (21.28% vs. 18.19% Supporting Information Fig. 4). By 13 days after differentiation, TuJ1⁺ neurons decreased to 10% in the control group (7.4% vs. 17.19%), whereas most Bcl-xL-infected cells survived (Supporting Information Fig. 4), suggesting that Bcl-xL overexpression primarily promotes the survival of SCZ-derived neuroblasts. Bcl-xL overexpression did not substantially alter the distribution of their progeny glial cells (Supporting Information Fig. 5).

Next, we examined whether the reduction of DCX⁺ neuroblasts in the Bcl-xL-injected group was accompanied by the increase of mature neurons. In striking contrast to the control group in which there was few, if any, newly produced NeuN⁺ mature neurons, we were able to detect a small but substantial number of NeuN⁺ cells expressing GFP in the Bcl-xL-infected group (Fig. 4D–4F). The numbers of GFP⁺/NeuN⁺ cells were similar when brain sections were examined at 30 and 90 day after TBI (TBI30D: 2 ± 1.1 cells, TBI90D: 1.75 ± 1.3 cells) (Fig. 4D–4F), suggesting that the majority of Bcl-xL-injected cells failed to differentiate into mature neurons.

We observed that the morphology of GFP⁺/NeuN⁺ cells was atypical and resembled atrophied neurons [8, 33, 34] in that the soma size of GFP⁺/NeuN⁺ cells was substantially smaller than normal NeuN-expressing neurons (11.7 ± 0.2 vs. 7.1 ± 0.4 μ m in diameter) (Fig. 4G), and that many GFP⁺/NeuN⁺ cells failed to develop neuronal processes (Fig. 4D, 4E). Taken together, Bcl-xL overexpression in SCZ-aNSCs increased the number of neuroblasts, but such cells failed to differentiate into mature neurons.

Atrophy of SCZ-Derived Neurons After Bcl-xL Overexpression

We often observed atrophied cells in the Bcl-xL virus-infected, but not in the control group (Fig. 5A). Double labeling of GFP and cell type-specific markers, such as GFAP, MBP, and NeuN, showed that none of such markers were detected in the atrophied cells (Fig. 5B). Instead, a subset of GFP⁺ atrophied cells

was labeled with DCX, suggesting that atrophied cells were derived from neuroblasts (Fig. 5C). On the basis of DCX expression and morphology, atrophied cells were categorized into three groups: (a) DCX⁺ cells with long processes (DCX⁺ normal cells), (b) DCX⁺ cells without processes (DCX⁺ atrophied cells), and (c) small cells without DCX expression (DCX⁻ atrophied cells). When observed at 30 days after TBI, DCX⁺ or DCX⁻ atrophied cells were readily detected in Bcl-xL-infected group. Interestingly, the reduction of DCX⁺ normal cells that occurred between 30 and 90 days after TBI was accompanied by the increase of DCX⁻ atrophied cells (Fig. 5D). These results favor the hypothesis that neuroblasts saved from apoptosis by Bcl-xL overexpression underwent growth arrest and progressively cell atrophy.

To obtain direct evidence that DCX⁻ atrophied cells are originated from DCX⁺ cells, we generated *DCX-creER* mice in which creER is exclusively expressed in DCX-expressing cells, including cells in the SCZ (Supporting Information Fig. 6). Detailed procedures for the generation of mouse and basic characterization of expression patterns are described in Supporting Information Materials. These DCX-creER mice were crossed with Rosa-EGFP reporter mice. Tamoxifen was injected daily for 5 consecutive days starting from the day when Bcl-xL virus was injected, and mice were subjected to TBI on the 2nd day of tamoxifen injection (Fig. 5E). When we examined brain sections 29 days after TBI, we found that Bcl-xL-expressing, GFP⁺ atrophied cells did not express DCX, confirming that such atrophied cells had lost their DCX expression (Fig. 5E). It has recently been reported that DCX expressing cells in the SVZ can trans-differentiate into oligodendrocytes in response to white matter injury [35]. However, none of the oligodendrocytes were labeled with GFP (Fig. 5E), ruling out the possibility that SCZ-derived DCX⁺ cells trans-differentiated into oligodendrocytes. Collectively, these results suggest that most Bcl-xL-overexpressing, DCX⁺ neuroblasts show atrophy, and only a limited proportion of cells harbor the capacity to differentiate and express NeuN.

BDNF Infusion in Combination with Bcl-xL Viral Infection Enhances Neuronal Maturation

Results described so far suggest that suppression of apoptosis is insufficient to promote neuronal maturation, and additional factors are required. Given that neurotrophic factors have been shown to enhance the growth/hypertrophy of atrophied neurons [36, 37], we tested whether infusion of BDNF into the injured cortex could rescue neurons from atrophy (Fig. 6). Treatment with BDNF every 3 days for a total of 30 days (total 10 injections) markedly increased the number of NeuN⁺ cells in Bcl-xL-infected group (Bcl-xL⁺/BDNF) as compared to CSF-treated group (Bcl-xL⁺/CSF) (Fig. 6A–6C). Moreover, such NeuN⁺ cells in the Bcl-xL⁺/BDNF group had large soma, indistinguishable to mature NeuN⁺ neurons (normal NeuN⁺ neurons: 11.34 ± 0.79 vs. NeuN⁺/Bcl-xL⁺/BDNF: 11.14 ± 1.13 μ m in diameter) and developed extensive neurites (Fig. 6B, inset). However, BDNF treatment alone was insufficient to produce NeuN⁺ cells in GFP-infected group (Fig. 6C), suggesting that both BDNF treatment and prevention of apoptotic cells death by Bcl-xL infection are required.

We next explored whether SCZ-derived neurons produced by Bcl-xL overexpression and BDNF infusion exhibited cortical neuronal phenotype. When we examined the expression of

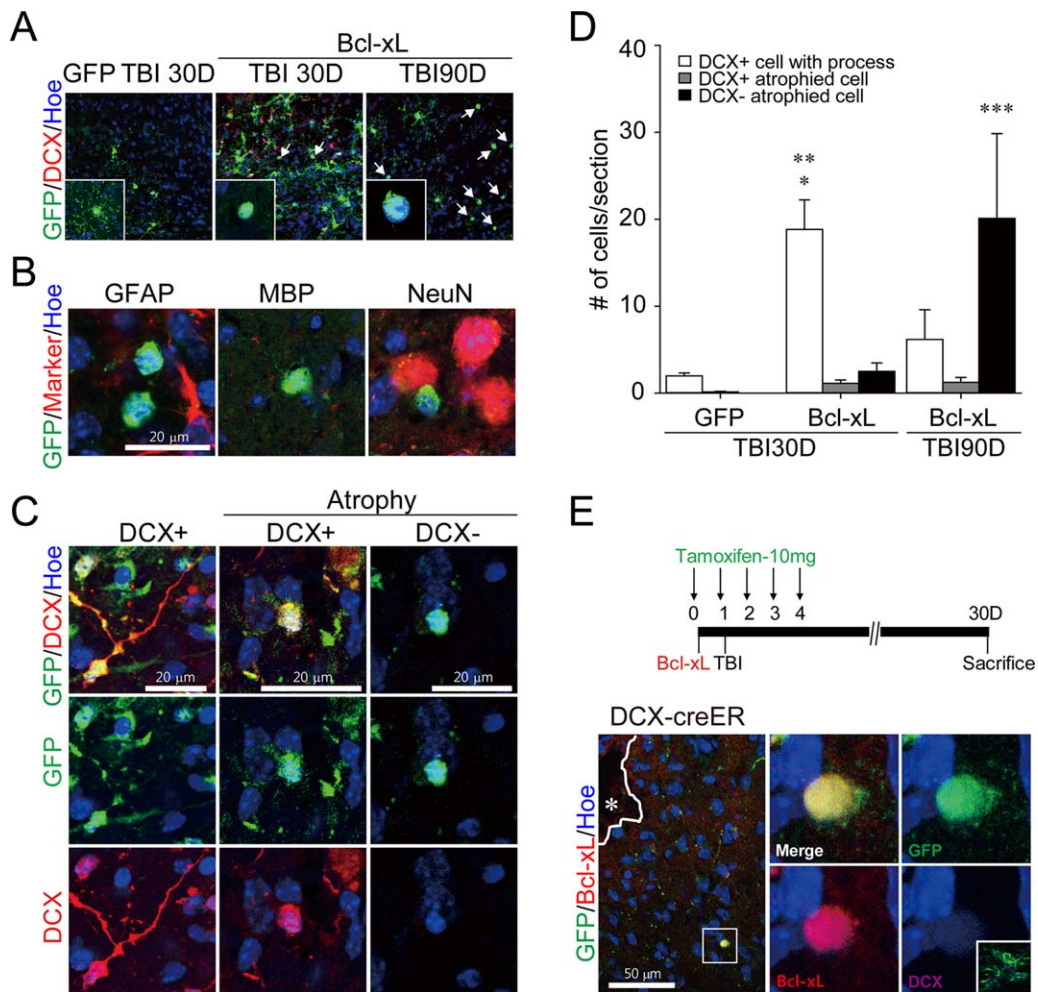


Figure 5. Atrophy of neuroblasts after Bcl-xL overexpression. **(A):** Representative images of atrophied cells detected from injured brains that had been infected with green fluorescent protein (GFP) or GFP-Bcl-xL at 30 and 90 days before traumatic brain injury (TBI). When observed at 30 days after TBI, most DCX⁺ cells in the Bcl-xL-transfected brain harbored multiple branches (left), whereas DCX⁺ cells in the Bcl-xL-transfected brain exhibited atrophied cell morphology characterized by round soma without branches. Arrows indicate atrophied cells. Insets show typical image of a cell in the GFP- or GFP-Bcl-xL-infected brain. **(B):** Representative images of atrophied cells in the injured, Bcl-xL-transfected brain. Brains were sectioned at 30 days after TBI and immunostained for glial fibrillary acidic protein (left), NeuN (middle), or myelin basic protein (right), as indicated. **(C):** Representative images of normal or atrophied cells from brains sectioned at 90 days after TBI. Brain sections were immunostained for DCX. Based on their morphology and DCX expression, Bcl-xL-infected cells were classified into following categories: DCX⁺ cells with processes, atrophied cells positive for DCX, and atrophied cells negative for DCX. Scale bar = 20 μ m. **(D):** Quantification of cell types. Data are expressed as mean \pm SEM ($n = 5$ for GFP group, $n = 8$ for Bcl-xL group). *, $p < 0.05$, Student's t test. (*, DCX + atrophied cells in GFP-TBI30D vs. DCX + cell with process in Bcl-xL-TBI30D; **, DCX- atrophied cells in GFP-TBI30D vs. DCX + cell with process in Bcl-xL-TBI30D; ***, DCX- atrophied cells in GFP-TBI30D vs. DCX- atrophied cells in Bcl-xL-TBI90D). **(E):** Fate tracing of Bcl-xL-expressing cells using DCX-tamoxifen-dependent Cre recombinase mouse. Experimental scheme (up) and representative images (down) are shown. Atrophied cells expressing Bcl-xL-dsRed (red) exhibited GFP signal, but DCX expression was not detected. Asterisk indicates injury core. Magnified images of an atrophied cell are shown on the right panels. Inset in the DCX channel (lower right) shows labeling of DCX in the subcallosal zone, but not in GFP-labeled cells. Nuclei were counter-stained with Hoechst 33342 (blue). Abbreviations: DCX, Doublecortin; GFAP, glial fibrillary acidic protein; GFP, green fluorescent protein; MBP, myelin basic protein; TBI, traumatic brain injury.

several markers for cerebral cortex neurons, we found that approximately 50% of NeuN⁺ neurons expressed Cux1 (marker for cortical layer II-IV neurons) (Bcl-xL⁺/CSF: 0.42 ± 0.07 vs. Bcl-xL⁺/BDNF: 2.33 ± 0.7 cells per section) or Tbr2 (marker for early glutamatergic neuron) (Bcl-xL⁺/CSF: 0 vs. Bcl-xL⁺/BDNF: 2.42 ± 0.82) (Fig. 6D, 6E, 6H, 6I). However, NeuN⁺ neurons did not express FEZF2 (marker for cortical layer V neurons) or FOG2 (marker for cortical layer VI neurons) (Supporting Information Fig. 8). A subset of neurons generated by Bcl-xL infection and BDNF treatment exhibited

c-Fos labeling, a histological marker for neuronal excitation (Fig. 6F). Furthermore, dendritic processes were evident in such neurons, and vGluT puncta were closely associated (Fig. 6G), suggesting terminal differentiation of newly generated cortex neurons.

Finally, we tested whether such SCZ-derived neurons can survive in the cerebral cortex for extended periods without further support of BDNF. After a total of 4 weeks of BDNF infusion, BDNF infusion was discontinued and the animals were killed 1- or 2-months later. We were able to detect

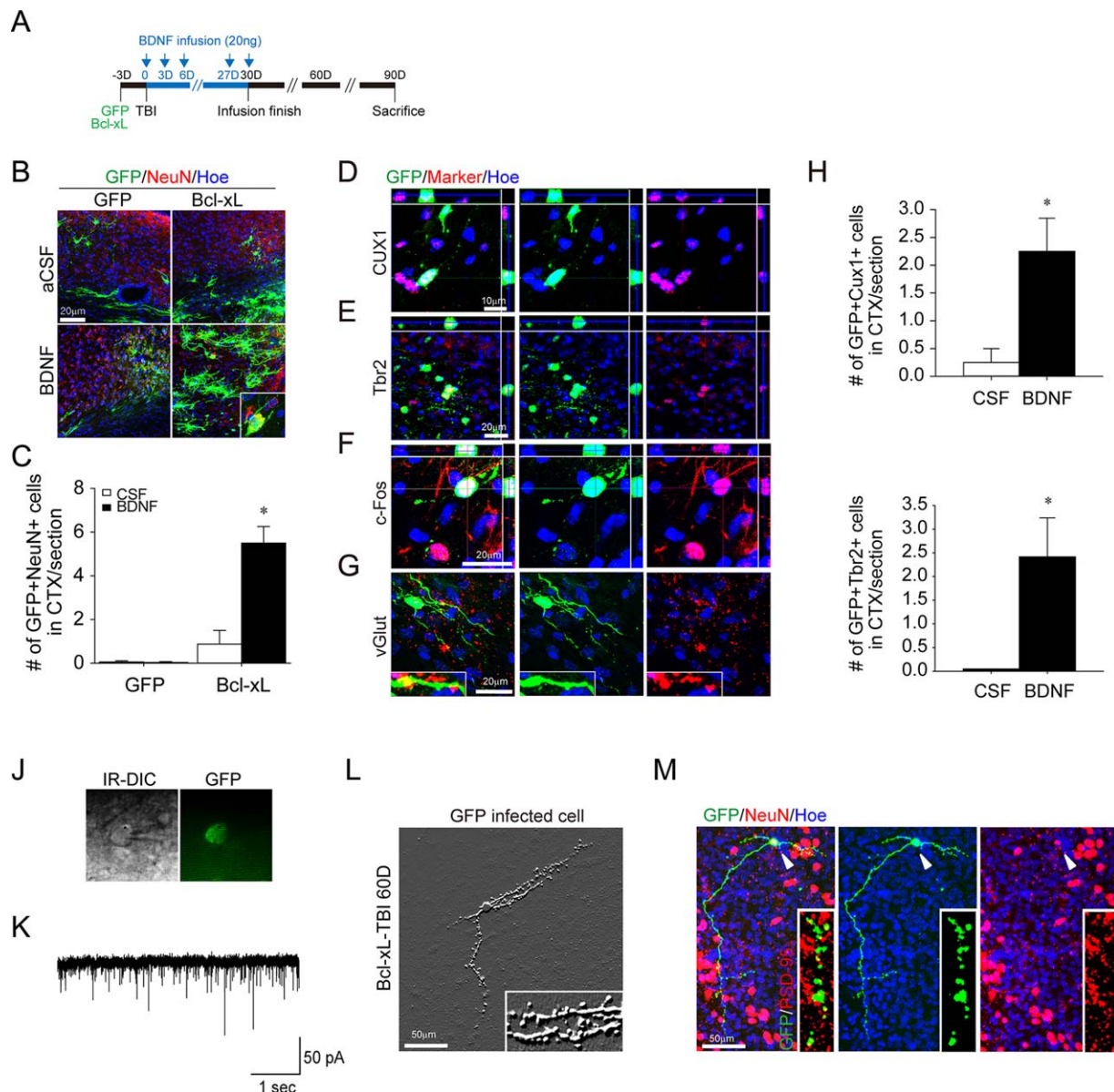


Figure 6. Subcallosal zone (SCZ)-derived neural stem cells receive synaptic input and exhibit mature neuronal morphology in response to brain-derived neurotrophic factor (BDNF) infusion. **(A)**: Experimental scheme of infection (green fluorescent protein [GFP] or GFP-Bcl-xL), traumatic brain injury (TBI), infusion with BDNF, and examination. After intracranial injection with GFP- or GFP-Bcl-xL-expressing retrovirus, mice were subjected to TBI and multiple infusions with BDNF (20 ng/3 days), as indicated. For electrophysiological analysis, mice were killed at 30 or 60 days after the last BDNF infusion. **(B)**: Representative images of brain sections from mice that had been subjected to TBI and infusion either with artificial cerebrospinal fluid (aCSF) or BDNF. Before TBI, either GFP- or GFP-Bcl-xL-expressing retrovirus was injected. Brain sections were examined at 30 days after TBI. Note that many GFP-Bcl-xL-overexpressing cells remained in the injured cortex when BDNF was infused. Scale bar = 20 μm **(B)**. **(C)**: Quantification of NeuN⁺ cells in the injured cortex examined from brain sections of mice infected with GFP- or GFP-Bcl-xL-expressing retrovirus. Data are expressed as mean ± SEM ($n = 3$ for GFP group, $n = 4$ for Bcl-xL group). *, $p < 0.05$ compared with CSF-infused group, Student's t test. **(D–G)**: Brains from GFP-Bcl-xL-transfected and BDNF-infused mice were sectioned and examined for Cux1 (a marker for cortical layer II–III cells, Scale bar = (D) 10 μm. (D), Tbr2 (a marker for early glutamatergic neurons, Scale bar = (E) 20 μm. (E), c-Fos (a marker for neuronal activity, Scale bar = (F) 20 μm. (F), and v-Glut (a marker for presynaptic glutamatergic neuron, Scale bar = (G) 20 μm (G) as indicated. **(H, I)**: Quantification of cells expressing Cux1 (H) and Tbr2 (I). Data are expressed as mean ± SEM ($n = 4$). *, $p < 0.05$, Student's t test. **(J)**: Infrared-differential interference microscopy and fluorescent images of the GFP-Bcl-xL-expressing cells. **(K)**: Spontaneous bursts from a GFP-Bcl-xL-expressing cell in brain slices prepared at 60 days after the last BDNF infusion (i.e. 90 days after TBI). **(L)**: Morphology of an SCZ-derived neuron that survived for 60 days after TBI. Brains infected with GFP-Bcl-xL-expressing retrovirus were subjected to TBI, followed by multiple BDNF infusions, as depicted in A. Brain section was fixed after electrophysiological analysis, and then immunostained for GFP. Signals were visualized with embossing images. Inset shows spine-like protrusions in dendrites. Scale bar = (L) 50 μm **(M)**: Images of a neuron expressing NeuN and GFP obtained at 90 days after TBI show elongated axons. Insets show that axonal boutons are juxtapositioned with post-synaptic structures labeled by PSD95. Arrowheads indicate NeuN-labeled cell body of the GFP-Bcl-xL-expressing neuron. Nuclei were counter-stained with Hoechst 33342 (blue). Scale bar = 50 μm (M). Abbreviations: aCSF, artificial cerebrospinal fluid; BDNF, brain-derived neurotrophic factor; CSF, cerebrospinal fluid; CTX, cortex; GFP, green fluorescent protein; IR-DIC, infrared-differential interference microscopy; TBI, traumatic brain injury.

spontaneous post-synaptic currents in the GFP-expressing cells in the brain slice 90 days after Bcl-xL-infection and BDNF infusion (Fig. 6J, 6K), suggesting that SCZ-derived cells received inputs (Fig. 6K). Furthermore, 1 month after the last BDNF infusion most neurons showed mature morphology with highly elongated axons and complex arborization of dendrites (Fig. 6L, 6M). Dendrites possessed spine-like structures, suggestive of post-synaptic specialization of excitatory synapses (Fig. 6L). In NeuN⁺ neurons with highly elongated axons (Fig. 6M), we observed that axonal boutons were closely associated with PSD95 puncta (postsynaptic marker) (Fig. 6M, inset). Collectively, these data suggest that SCZ-derived neurons generated by Bcl-xL-infection and BDNF infusion obtained electrophysiological and morphological properties of mature neurons.

DISCUSSION

The SCZ is a unique adult brain region where multipotent aNSCs are localized and spontaneously produce new neuroblasts. However, under normal conditions, little, if any, neurons survive due to massive programmed cell death (PCD) [8]. This study compares the potential of SCZ-aNSCs to proliferate and differentiate with that of SVZ-aNSCs and reports that SCZ-aNSCs exhibit weaker neurogenic potential than SVZ-aNSCs in culture. It is known that NSCs in the SVZ are anatomically organized in a mosaic-like pattern and that NSCs in each microdomain produce a distinct subpopulation of olfactory bulb neurons [28, 38]. SCZ is originated from the posterior domain of embryonic lateral ventricle [16], and their distinct properties can be explained by a mosaic-like arrangement of NSCs along the anterior-posterior axis of the lateral ventricle. In normal brain, NSCs in the SCZ mainly produce oligodendrocytes. Neuroblasts are also generated, but eventually undergo apoptosis and fail to migrate to the olfactory bulb [8]. Therefore, the limited neurogenic potential of SCZ-derived NSCs that we observed in culture appears to reflect their *in vivo* activities.

Transplantation of the SCZ-aNSCs into the adult SVZ also demonstrated significant but limited ability for neurogenesis. Previously, it was reported that the SCZ-derived NSCs failed to produce neurons in the cerebral cortex after transplantation [16]. Similarly, NSCs derived from the temporal subcortical white matter, an anatomical area associated with SCZ, fail to undergo neuronal differentiation in the rat cerebral cortex after xenograft [19]. Because transplantation of NSCs into the non-neurogenic area such as cerebral cortex showed limited neuronal differentiation [39], we grafted SCZ-aNSCs into a permissive environment in SVZ. Within the SVZ, NSCs derived from SCZ differentiated to multiple lineages of neural cells including neurons and glia, further confirming their multiple potential *in vivo*. However, compared with the SVZ-aNSCs, SCZ-aNSCs produced less neuroblasts, which might be associated with their limited neurogenic potential.

Previously, we have revealed that the NSCs in the SCZ preferentially respond to posterior cortical injury, whereas NSCs in the SVZ mainly respond to anterior cortical damage [8]. However, to the best of our knowledge, there has been no report regarding the long-term responses of SCZ-aNSCs to brain injury. Here we have examined the long-term fate of

SCZ-derived neuroblasts after focal brain damage and suggest methods to promote their functional maturation *in vivo*. Following brain injury, aNSCs in the SCZ initially produce all major neural cell types including neuroblasts, astrocytes, and oligodendrocytes. Among such multiple cell types, neuroblasts failed to survive, whereas astrocytes and oligodendrocytes were maintained in the injured cerebral cortex. In normal brain, aNSCs in the SCZ produce oligodendrocytes needed for postnatal myelination in the white matter [40, 41]. It is known that brain trauma promotes the expansion of astrocytes in the injury penumbra region [8], and it appears that the NSCs in the SCZ contribute to the generation of astrocytes and oligodendrocytes following brain injury. However, injured cerebral cortex exhibit limited potential to incorporate the newly added SCZ-derived neurons into the existing neural circuitry. Several reports have demonstrated that neurogenesis can be induced in the cerebral cortex following TBI [8, 42–45] or stroke [46–50]. Cerebral cortex contains widely distributed local neurogenic progenitor cells, which may be produced from reactive astrocytes [45, 51, 52]. Because our experiment cannot rule out the possibility that new neurons could be generated from such local precursors, it remains unclear to what extent posterior TBI promotes cortical neurogenesis.

Neuroblasts expressing DCX differentiated from the SCZ-aNSCs underwent apoptosis. Previously, we demonstrated that the death of the SCZ-derived neuroblasts depends on the activation of a pro-apoptotic gene *bax* [8]. Because Bcl-xL strongly suppresses *bax* gene function, retrovirus-encoding Bcl-xL was injected into the SCZ to prevent cell death. The prevention of cell death by Bcl-xL overexpression increased the number of DCX-expressing neuroblasts (e.g., 1-month after TBI compared with 7 days; Fig. 4B, 4C), indicating that Bcl-xL prevented apoptosis of proliferating progenitors, which can produce DCX⁺ neuroblasts. Accompanied by the prevention of apoptosis, a small subset of neuroblasts differentiated into mature, NeuN⁺ neurons, however, most neurons expressing NeuN were morphologically unusual, with no or few neuronal processes, suggesting that neuronal maturation program was not fully activated. In fact, the number of cells expressing NeuN at 60 days was less than 5% when compared with the number of DCX-expressing cells at peak period (30 days) (Fig. 4B, 4C). Instead, there was an increase in the atrophied cell population, characterized morphologically by their small soma and round shape. In these cells, none of the markers used in this study were detected. Lineage tracing using DCX-creER mice confirmed our conclusion that most Bcl-xL-expressing neuroblasts, which escaped apoptosis, became eventually atrophied. Of note, atrophy coupled with prevention of neuronal maturation was also observed in many neuronal populations of *bax*-knockout (KO) mice [8, 34, 53, 54]. For instance, motoneurons or Purkinje cells that escaped developmental PCD by *bax* deletion failed to maintain their original connectivity or localization and atrophied extensively [34, 54]. Furthermore, SCZ-derived neuroblasts in *bax*-KO mice also underwent atrophic changes in normal, intact brain [8]. These results suggest that prevention of neuronal death does not lead to maturation of survived neurons by default, and additional signals are required for the maturation and functional integration of new-borne neurons in the cerebral cortex.

We have demonstrated that the supplement of BDNF rescues neurons from atrophy. It has been shown that postnatal treatment with GDNF promotes re-innervation and hypertrophy of atrophied motoneurons [55] and that treatment of BDNF promotes neuronal differentiation in the SCZ in the absence of brain injury in wildtype or *bax*-KO mice [8]. Furthermore, treatment of BDNF was necessary for neuronal maturation following *in situ* transdifferentiation of glial cells into neuroblasts [56], suggesting the importance of BDNF signals for neuronal maturation in adult brain. Therefore, we tested whether atrophy of SCZ-derived neurons in the injured cortex could be rescued by BDNF treatment. While BDNF infusion alone failed to promote neuronal differentiation, combination of BDNF and Bcl-xL overexpression markedly increased the number of SCZ-derived mature neurons. Interestingly, such SCZ-derived mature neurons expressed markers for cortical neurons. At least one marker for superficial layer II-III cortical neurons, CUX1 [57], was detected in the SCZ-derived neurons. Superficial layer cortical neurons are late-borne neurons generated during embryonic development, and aNSCs appear to preferentially produce such late-borne neurons *in vivo*. In addition to NeuN expression, these SCZ-derived neurons exhibited early signs of neuronal maturation, such as arborization of dendritic processes, cell hypertrophy, and provisional synaptic contacts supported by Tbr2 and vGlut staining.

Considering that either Bcl-xL or BDNF alone failed to promote neuronal maturation, it appears that these two factors synergistically act on different processes of neuronal maturation (Fig. 6A–6C). We observed that Bcl-xL prevents rapid death of neuroblasts, and BDNF primarily promotes process arborization and synaptic integration into mature circuits. BDNF is well known to play critical roles in synapse formation [44, 58, 59], and synaptic integration is necessary for the long-term survival of neurons [60]. Therefore, enforcement of synaptic integration with the addition of neurotrophic factors might be required for neuronal maturation. During the development of the nervous system, it is well established that a critical period exists for the survival and synaptic integration of newly produced neurons in neurogenic regions [61, 62]. Therefore, it is plausible to suggest that addition of BDNF elicits better effects if applied during a critical period after injury in adult brain. Interestingly, we observed that 1–4 weeks of BDNF application after injury was sufficient to induce long-term survival and continuous maturation of SCZ-derived neurons in the injured cortex. By 2 months after the final BDNF infusion, SCZ-derived neurons appeared more mature with dendritic spine-like protrusions. Given the many roles of BDNF in the nervous system, prolonged infusion of BDNF might not always be beneficial and cause aversive effects including neuronal death [63] and ectopic synapse formations [64]. Thus, future studies should determine optimal time/duration of BDNF treatment to provide a safe, reliable, and economical strategy for brain repair.

In this study, we report that SCZ-aNSC can be engineered to generate mature neurons by prevention of apoptosis and treat-

ment of BDNF, but it should be noted that approximately 50%–70% SCZ-derived neurons remained atrophied. Several reports have suggested that the absence of appropriate neurogenic signals or the presence of inhibitory signals might present challenges to cortical neurogenesis [65]. Sonic hedgehog (Shh) is one of the factors enriched in the neurogenic regions, and the addition of Shh into the cerebral cortex promoted neuronal differentiation from transplanted NSCs [66, 67], which would otherwise differentiate into astrocytes or oligodendrocytes [68]. Therefore, other factors may also contribute to the regulation of neuronal maturation in the injured brain, and combination of pertinent factors might promote more robust neuronal maturation.

CONCLUSION

In summary, we demonstrate that mature neurons can be generated from SCZ-aNSCs by prevention of apoptosis and neurotrophic treatment. SCZ-aNSCs showed weaker neurogenic potential than SVZ-aNSCs *in vitro* and *in vivo* system. Few neurons differentiated from SCZ-aNSCs survive and mature under TBI condition. Combination of Bcl-xL overexpression and BDNF infusion rescue newborn neurons from cell death and atrophy. Taken together, our results suggest that SCZ-aNSCs might be a potential source of cells for cortical neurogenesis-based brain repair.

ACKNOWLEDGMENTS

We thank Dr. Eun Mi Hur at Korea Institute of Science and Technology for critical reading of the manuscript and Dr. Magdalena Götz for providing us CAG-GFP-IRES-DsRed. This work was supported by the Brain Research Program through the National Research Foundation (NRF) funded by the Korean Ministry of Science, ICT, and Future Planning (Grants NRF-2012M3A9C6049933, NRF-2010-0020237, NRF-2015M3C7A1028790, and NRF-2013R1A1A3011896).

AUTHOR CONTRIBUTIONS

J.Y.K.: collection and/or assembly of data, data analysis and interpretation, manuscript writing; K.C., M.R.S., J.-H.L., B.L., and E.L.: collection and/or assembly of data; J.-Y.P. and K.S.S.: data analysis and interpretation; M.-S.L. and C.H.P.: provision of study material or patients; H.K.: provision of study material or patients, conception and design; D.G.: final approval of manuscript, provision of study material or patients, manuscript writing, conception and design; W.S.: final approval of manuscript, manuscript writing, conception and design, collection and/or assembly of data, financial support.

POTENTIAL CONFLICTS OF INTEREST

The authors indicate no potential conflicts of interest.

REFERENCES

- Gould E. How widespread is adult neurogenesis in mammals? *Nat Rev Neurosci* 2007;8:481–488.
- Ohira K. Injury-induced neurogenesis in the mammalian forebrain. *Cell Mol Life Sci* 2011;68:1645–1656.
- Sun X, Zhang QW, Xu M et al. New striatal neurons form projections to substantia nigra in adult rat brain after stroke. *Neurobiol Dis* 2012;45:601–609.
- Moon Y, Kim JY, Kim WR et al. Function of ezrin-radixin-moesin proteins in migration of subventricular zone-derived neuroblasts

following traumatic brain injury. *STEM CELLS* 2013;31:1696–1705.

- 5 Collin T, Arvidsson A, Kokaia Z et al. Quantitative analysis of the generation of different striatal neuronal subtypes in the adult brain following excitotoxic injury. *Exp Neurol* 2005;195:71–80.
- 6 Kernie SG, Parent JM. Forebrain neurogenesis after focal ischemic and traumatic brain injury. *Neurobiol Dis* 2010;37:267–274.
- 7 Kojima T, Hirota Y, Ema M et al. Subventricular zone-derived neural progenitor cells migrate along a blood vessel scaffold toward the post-stroke striatum. *STEM CELLS* 2010;28:545–554.
- 8 Kim WR, Chun SK, Kim TW et al. Evidence for the spontaneous production but massive programmed cell death of new neurons in the subcallosal zone of the postnatal mouse brain. *Eur J Neurosci* 2011;33:599–611.
- 9 Magavi SS, Leavitt BR, Macklis JD. Induction of neurogenesis in the neocortex of adult mice. *Nature* 2000;405:951–955.
- 10 Toni N, Sultan S. Synapse formation on adult-born hippocampal neurons. *Eur J Neurosci* 2011;33:1062–1068.
- 11 Quadrato G, Elnaggar MY, Di Giovanni S. Adult neurogenesis in brain repair: Cellular plasticity vs. cellular replacement. *Front Neurosci* 2014;8:17.
- 12 Jessberger S, Gage FH. Adult neurogenesis: Bridging the gap between mice and humans. *Trends Cell Biol* 2014;24:558–563.
- 13 Eriksson PS, Perfilieva E, Bjork-Eriksson T et al. Neurogenesis in the adult human hippocampus. *Nat Med* 1998;4:1313–1317.
- 14 Hack MA, Saghatelian A, de Chevigny A et al. Neuronal fate determinants of adult olfactory bulb neurogenesis. *Nat Neurosci* 2005;8:865–872.
- 15 Lledo PM, Alonso M, Grubb MS. Adult neurogenesis and functional plasticity in neuronal circuits. *Nat Rev Neurosci* 2006;7:179–193.
- 16 Seri B, Herrera DG, Gritti A et al. Composition and organization of the SCZ: A large germinal layer containing neural stem cells in the adult mammalian brain. *Cereb Cortex* 2006;16 Suppl 1:i103–111.
- 17 Kim HJ, Kim JY, Sun W. Age-dependent changes in the subcallosal zone neurogenesis of mice. *Neurochem Int* 2012;61:879–884.
- 18 Takemura NU. Evidence for neurogenesis within the white matter beneath the temporal neocortex of the adult rat brain. *Neuroscience* 2005;134:121–132.
- 19 Nunes MC, Roy NS, Keyoung HM et al. Identification and isolation of multipotential neural progenitor cells from the subcortical white matter of the adult human brain. *Nat Med* 2003;9:439–447.
- 20 Suarez-Sola ML, Gonzalez-Delgado FJ, Pueyo-Morlans M et al. Neurons in the white matter of the adult human neocortex. *Front Neuroanat* 2009;3:7.
- 21 Judas M, Sedmak G, Pletikos M et al. Populations of subplate and interstitial neurons in fetal and adult human telencephalon. *J Anat* 2010;217:381–399.
- 22 Jovanov-Milosevic N, Petanjek Z, Petrovic D et al. Morphology, molecular phenotypes and distribution of neurons in developing human corpus callosum. *Eur J Neurosci* 2010;32:1423–1432.
- 23 Kostovic I, Rakic P. Cytology and time of origin of interstitial neurons in the white matter in infant and adult human and monkey telencephalon. *J Neurocytol* 1980;9:219–242.
- 24 Nakatomi H, Kuriu T, Okabe S et al. Regeneration of hippocampal pyramidal neurons after ischemic brain injury by recruitment of endogenous neural progenitors. *Cell* 2002;110:429–441.
- 25 Jung AR, Kim TW, Rhyu IJ et al. Misplacement of Purkinje cells during postnatal development in Bax knock-out mice: A novel role for programmed cell death in the nervous system? *J Neurosci* 2008;28:2941–2948.
- 26 Kim WR, Kim Y, Eun B et al. Impaired migration in the rostral migratory stream but spared olfactory function after the elimination of programmed cell death in Bax knock-out mice. *J Neurosci* 2007;27:14392–14403.
- 27 Sun W, Winseck A, Vinsant S et al. Programmed cell death of adult-generated hippocampal neurons is mediated by the proapoptotic gene Bax. *J Neurosci* 2004;24:11205–11213.
- 28 Merkle FT, Mirzadeh Z, Alvarez-Buylla A. Mosaic organization of neural stem cells in the adult brain. *Science* 2007;317:381–384.
- 29 Dash PK, Mach SA, Moore AN. Enhanced neurogenesis in the rodent hippocampus following traumatic brain injury. *J Neurosci Res* 2001;63:313–319.
- 30 Komitova M, Mattsson B, Johansson BB et al. Enriched environment increases neural stem/progenitor cell proliferation and neurogenesis in the subventricular zone of stroke-lesioned adult rats. *Stroke* 2005;36:1278–1282.
- 31 Parent JM. Injury-induced neurogenesis in the adult mammalian brain. *Neuroscientist* 2003;9:261–272.
- 32 Chang MY, Sun W, Ochiai W et al. Bcl-XL/Bax proteins direct the fate of embryonic cortical precursor cells. *Mol Cell Biol* 2007;27:4293–4305.
- 33 Sun W, Oppenheim RW. Response of motoneurons to neonatal sciatic nerve axotomy in Bax-knockout mice. *Mol Cell Neurosci* 2003;24:875–886.
- 34 Jung AR, Kim TW, Rhyu IJ et al. Misplacement of Purkinje cells during postnatal development in Bax knock-out mice: A novel role for programmed cell death in the nervous system? *J Neurosci* 2008;28:2941–2948.
- 35 Jablonska B, Aguirre A, Raymond M et al. Chordin-induced lineage plasticity of adult SVZ neuroblasts after demyelination. *Nat Neurosci* 2010;13:541–550.
- 36 Sinson G, Perri BR, Trojanowski JQ et al. Improvement of cognitive deficits and decreased cholinergic neuronal cell loss and apoptotic cell death following neurotrophin infusion after experimental traumatic brain injury. *J Neurosurg* 1997;86:511–518.
- 37 Andsberg G, Kokaia Z, Klein RL et al. Neuropathological and behavioral consequences of adeno-associated viral vector-mediated continuous intrastriatal neurotrophin delivery in a focal ischemia model in rats. *Neurobiol Dis* 2002;9:187–204.
- 38 Merkle FT, Fuentealba LC, Sanders TA et al. Adult neural stem cells in distinct microdomains generate previously unknown interneuron types. *Nat Neurosci* 2014;17:207–214.
- 39 Herrera DG, Garcia-Verdugo JM, Alvarez-Buylla A. Adult-derived neural precursors transplanted into multiple regions in the adult brain. *Ann Neurol* 1999;46:867–877.
- 40 Windrem MS, Roy NS, Wang J et al. Progenitor cells derived from the adult human subcortical white matter disperse and differentiate as oligodendrocytes within demyelinated lesions of the rat brain. *J Neurosci Res* 2002;69:966–975.
- 41 Menn B, Garcia-Verdugo JM, Yaschine C et al. Origin of oligodendrocytes in the subventricular zone of the adult brain. *J Neurosci* 2006;26:7907–7918.
- 42 Covey MV, Jiang Y, Alli VV et al. Defining the critical period for neocortical neurogenesis after pediatric brain injury. *Dev Neurosci* 2010;32:488–498.
- 43 Vessal M, Darian-Smith C. Adult neurogenesis occurs in primate sensorimotor cortex following cervical dorsal rhizotomy. *J Neurosci* 2010;30:8613–8623.
- 44 Alsina B, Vu T, Cohen-Cory S. Visualizing synapse formation in arborizing optic axons in vivo: Dynamics and modulation by BDNF. *Nat Neurosci* 2001;4:1093–1101.
- 45 Shimada IS, LeComte MD, Granger JC et al. Self-renewal and differentiation of reactive astrocyte-derived neural stem/progenitor cells isolated from the cortical peri-infarct area after stroke. *J Neurosci* 2012;32:7926–7940.
- 46 Jiang W, Gu W, Brannstrom T et al. Cortical neurogenesis in adult rats after transient middle cerebral artery occlusion. *Stroke* 2001;32:1201–1207.
- 47 Parent JM, Vexler ZS, Gong C et al. Rat forebrain neurogenesis and striatal neuron replacement after focal stroke. *Ann Neurol* 2002;52:802–813.
- 48 Jin G, Omori N, Li F et al. Protection against ischemic brain damage by GDNF affecting cell survival and death signals. *Neurol Res* 2003;25:249–253.
- 49 Masuda T, Isobe Y, Aihara N et al. Increase in neurogenesis and neuroblast migration after a small intracerebral hemorrhage in rats. *Neurosci Lett* 2007;425:114–119.
- 50 Ziv Y, Finkelstein A, Geffen Y et al. A novel immune-based therapy for stroke induces neuroprotection and supports neurogenesis. *Stroke* 2007;38:774–782.
- 51 Ahmed AI, Shtaya AB, Zaben MJ et al. Endogenous GFAP-positive neural stem/progenitor cells in the postnatal mouse cortex are activated following traumatic brain injury. *J Neurotrauma* 2012;29:828–842.
- 52 Kreuzberg M, Kanov E, Timofeev O et al. Increased subventricular zone-derived cortical neurogenesis after ischemic lesion. *Exp Neurol* 2010;226:90–99.
- 53 Kim TW, Moon Y, Kim K et al. Dissociation of progressive dopaminergic neuronal death and behavioral impairments by Bax deletion in a mouse model of Parkinson's disease. *PLoS One* 2011;6:e25346.
- 54 Sun W, Gould TW, Vinsant S et al. Neuromuscular development after the prevention of naturally occurring neuronal death by Bax deletion. *J Neurosci* 2003;23:7298–7310.

- 55** Sun W, Winseck A, Vinsant S et al. Programmed cell death of adult-generated hippocampal neurons is mediated by the proapoptotic gene Bax. *J Neurosci* 2004;24:11205–11213.
- 56** Niu W, Zang T, Zou Y et al. In vivo reprogramming of astrocytes to neuroblasts in the adult brain. *Nat Cell Biol* 2013;15:1164–1175.
- 57** Ferrere A, Vitalis T, Gingras H et al. Expression of Cux-1 and Cux-2 in the developing somatosensory cortex of normal and barrel-defective mice. *Anat Rec A Discov Mol Cell Evol Biol* 2006;288:158–165.
- 58** McAllister AK, Lo DC, Katz LC. Neurotrophins regulate dendritic growth in developing visual cortex. *Neuron* 1995;15:791–803.
- 59** Bamji SX, Rico B, Kimes N et al. BDNF mobilizes synaptic vesicles and enhances synapse formation by disrupting cadherin-beta-catenin interactions. *J Cell Biol* 2006;174:289–299.
- 60** Rao MS, Hattiangady B, Shetty AK. Fetal hippocampal CA3 cell grafts enriched with FGF-2 and BDNF exhibit robust long-term survival and integration and suppress aberrant mossy fiber sprouting in the injured middle-aged hippocampus. *Neurobiol Dis* 2006;21:276–290.
- 61** Kim WR, Sun W. Programmed cell death during postnatal development of the rodent nervous system. *Dev Growth Differ* 2011;53:225–235.
- 62** Buss RR, Sun W, Oppenheim RW. Adaptive roles of programmed cell death during nervous system development. *Annu Rev Neurosci* 2006;29:1–35.
- 63** Frade JM, Rodriguez-Tebar A, Barde YA. Induction of cell death by endogenous nerve growth factor through its p75 receptor. *Nature* 1996;383:166–168.
- 64** Koyama R, Yamada MK, Fujisawa S et al. Brain-derived neurotrophic factor induces hyperexcitable reentrant circuits in the dentate gyrus. *J Neurosci* 2004;24:7215–7224.
- 65** Favaro R, Valotta M, Ferri AL et al. Hippocampal development and neural stem cell maintenance require Sox2-dependent regulation of Shh. *Nat Neurosci* 2009;12:1248–1256.
- 66** Machold R, Hayashi S, Rutlin M et al. Sonic hedgehog is required for progenitor cell maintenance in telencephalic stem cell niches. *Neuron* 2003;39:937–950.
- 67** Riquelme PA, Drapeau E, Doetsch F. Brain micro-ecologies: Neural stem cell niches in the adult mammalian brain. *Philos Trans R Soc Lond B Biol Sci* 2008;363:123–137.
- 68** Jiao J, Chen DF. Induction of neurogenesis in nonconventional neurogenic regions of the adult central nervous system by niche astrocyte-produced signals. *STEM CELLS* 2008;26:1221–1230.



See www.StemCells.com for supporting information available online.